

Mapping the Evolution of Optically-Generated Rotational Wavepackets in a Room Temperature Ensemble of D₂

W. A. Bryan,^{1,2,*} E. M. L. English,¹ J. McKenna,³ J. Wood,¹ C. R. Calvert,³ R. Torres,⁴ I. C. E. Turcu,² J. L. Collier,² I. D. Williams,^{3,†} and W. R. Newell^{1,‡}

¹*Department of Physics and Astronomy, University College London, Gower Street, London WC1E 6BT, UK*

²*Central Laser Facility, Rutherford Appleton Laboratory, Chilton, Didcot, Oxon OX11 0QX, UK*

³*Department of Pure and Applied Physics, Queen's University Belfast, Belfast BT7 1NN, UK*

⁴*Blackett Laboratory, Imperial College London, Prince Consort Road, London SW7 2BW, UK*

(Dated: February 1, 2008)

A coherent superposition of rotational states in D₂ has been excited by nonresonant ultrafast (12 femtosecond) intense (2×10^{14} Wcm⁻²) 800 nm laser pulses leading to impulsive dynamic alignment. Field-free evolution of this rotational wavepacket has been mapped to high temporal resolution by a time-delayed pulse, initiating rapid double ionization, which is highly sensitive to the angle of orientation of the molecular axis with respect to the polarization direction, θ . The detailed fractional revivals of the neutral D₂ wavepacket as a function of θ and evolution time have been observed and modelled theoretically.

PACS numbers: 42.50.Hz, 33.80.Gj, 33.80.Wz

The importance of being able to enforce spatial order on an initially random ensemble of molecules has been recognized since the discovery of steric effects in chemical reactions [1]. Traditional 'brute force' techniques employing strong DC fields [2, 3] have recently yielded to new, more subtle and yet more powerful and versatile techniques using intense laser systems [4, 5]. In particular intense femtosecond pulses have been successfully used to align molecules along an axis for application in areas such as the study of fragmentation dynamics [6, 7], high harmonic generation [8, 9] and the creation of single cycle laser pulses [10]. In this case the alignment of a molecule (or spatial ordering of an ensemble of molecules) evolves temporally following the creation of a rotational wavepacket by a linearly polarized laser pulse of far shorter duration than the natural period of rotation.

In this Letter, we report on a detailed ultrafast study of the temporal evolution of such a rotational wavepacket in the neutral deuterium molecule D₂. The wavepacket is created impulsively by a 12 femtosecond laser pulse, with temporal and angular ordering probed at some later time with a similar pulse that initiates sequential double ionization (SI) i.e. $D_2 \rightarrow D_2^+ \rightarrow D^+ + D^+$ [11]. Such high resolution measurements represent the state-of-the-art in ultrafast molecular physics in the high rotational frequency limit as dictated by this most fundamental and theoretically tractable of molecules.

It is known that an intense linearly polarized laser pulse interacting with an ensemble of molecules generates a degree of spatial alignment from a random ensemble [4, 5]. The only condition for this phenomenon is that the molecular polarizability is anisotropic. Thus, the induced dipole moment created in the interaction with the electric field of the laser generates a torque that causes the axis of maximum polarizability to librate around the

polarization vector of the laser field. Quantum mechanically, the process is described as a sequence of Rabi-type cycles accompanied by the exchange of two quanta of angular momentum between the molecule and the laser field. If the aligning pulse duration is much greater than the rotational period, the system evolves adiabatically to the so-called pendular states, which dissipate as soon as the laser pulse passes [12]. However, when the pulse duration is much shorter than the rotational period, a superposition of rotational states is created that outlives the laser pulse, and the phases in the rotational wavepacket continue to evolve [5]. As a consequence of the quantization of the J states, a periodic dephasing and rephasing of the wavepacket occurs in the field-free regime. At integer and half-integer multiples of $(2Bc)^{-1}$ (where B is the rotational constant and c is the speed of light in vacuum) a revival of the rotational wavepacket is expected, at which point the ensemble exhibits a significant degree of alignment, with the molecular axes parallel to the polarization vector of the initial pulse. The relative phases of the J states also produces antialignment in the ensemble, whereby the molecular axes are orientated to lie on or near the plane normal to the initial pulse polarization. Alignment and antialignment are well distinguished temporally. As a consequence of the nuclear spin statistics, homonuclear systems can also present partial revivals at 1/4 and 3/4 of the rotational period.

Previous observations of impulsive alignment have been restricted by the non-availability of laser pulses sufficiently shorter than the rotational periods. However, rotational wavepackets have been previously observed in heavy many-electron systems (N₂ [6], O₂ [13, 14], CO₂ [15, 16], CS₂ [16], I₂ [17] etc.), where rotations occur with periods on the picosecond time scale. The rotational revival in D₂ occurs at $(2Bc)^{-1} = 558$ fs, requiring an aligning pulse of the order of tens of femtoseconds in duration.

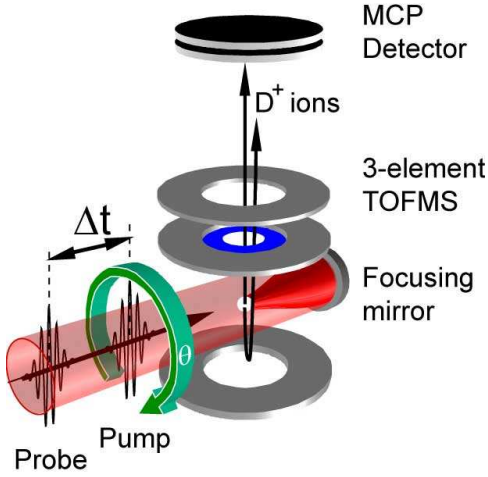


FIG. 1: The experimental configuration used to observe rotational wavepackets in D_2 imprinted on the D^+ rapid sequential ionization (SI) yield ($D_2 \rightarrow D_2^+ \rightarrow D^+ + D^+$) as measured with a time-of-flight mass spectrometer (TOFMS). The time delay between the pump and probe pulses is Δt , and the angle θ between pump and probe polarization directions is varied by rotating the pump polarization. As shown, $\theta = 0$.

Dynamic alignment of D_2 using 10 fs pulses has recently been demonstrated by Lee *et al* [18], however, these observations were of limited temporal resolution and the angular evolution of the rotational wavepacket was not measured.

In the present work, the spatio-temporal evolution of the D_2 rotational wavepacket has been simulated following the procedure described in [19]. Briefly, a thermal ensemble of rigid rotors is considered, each of which gives rise to a superposition of rotational states, $|\Psi_{J_i M_i}\rangle = \sum_{J \geq |M_i|} F_{J_i J}(t) |J M_i\rangle$ in which $F_{J_i J}(t)$ are the time-dependent complex coefficients (note that M_i is conserved in a linearly polarized field). These coefficients are calculated by numerically solving the time-dependent Schrödinger equation, and are used to calculate the thermal average of the degree of alignment and the angular evolution of the ensemble.

Due to the bosonic character of D_2 , the total wavefunction of the molecule must be symmetric under inversion. The electronic ground state is symmetric, and the nuclei can form six symmetric (ortho) and three antisymmetric (para) nuclear wavefunctions. This restricts the J states populated: para- D_2 occupies only odd J -states, and ortho- D_2 occupies only even J -states. This results in a 2 : 1 weighting (ortho- D_2 : para- D_2) in a thermal ensemble. For a room temperature sample we expect the following initial populations (in parenthesis) for the different J states: $J = 0$ (0.185), 1 (0.208), 2 (0.386), 3 (0.112), 4 (0.0899), 5 (0.0128) and 6 (0.00522).

The experiment was carried out using 800nm, 0.4 mJ, 10 fs pulses at 1 kHz repetition rate. The pulses were split by a 4 μm thick pellicle beamsplitter. A co-linear

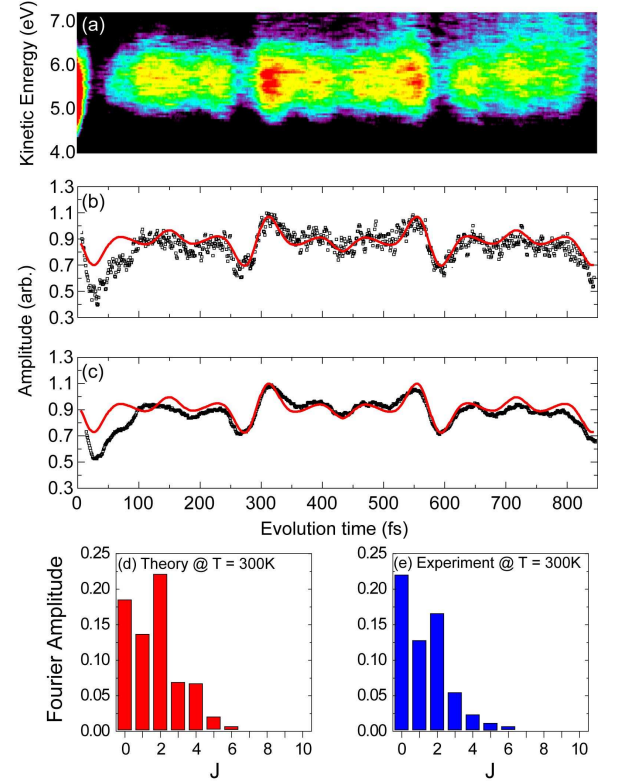


FIG. 2: (a) False colour representation of the D^+ rapid sequential ionization (SI) yield ($D_2 \rightarrow D_2^+ \rightarrow D^+ + D^+$) as a function of pump-probe delay (thus wavepacket evolution time) Δt and ion kinetic energy. (b) Integrated SI yield compared to theoretically predicted influence of an impulsively excited rotational wavepacket in D_2 (red). Throughout, $\theta = \pi/2$, see Fig. 1, and the step in $\Delta t = 1$ fs. (c) Integrated SI yield following an 11-point smoothing. The 1/4, 1/2 and 3/4 revivals are more clearly observed. Fourier Transform of the theoretical simulation and experimental SI yield are shown in (d) and (e) respectively. The frequency components present in the rotational wavepacket are beats between rotational states ΔJ and $\Delta J + 2$. The Fourier amplitudes thus return a measure of rotational population.

Mach-Zehnder interferometer configuration was used to delay the resulting 70 μJ , 12 fs probe pulse with respect to the 73 μJ , 12 fs pump pulse with 300 attosecond resolution [20]. A half-wave plate mounted in one arm of the interferometer allowed the pump polarization to be rotated through an angle θ with respect to the probe polarization, which was fixed parallel to the spectrometer axis. In comparison to the core-annulus method [18], the present technique does suffer greater energy loss in the split pulses. However, this is compensated by the temporal consistency of the spatial overlap at focus as a function of time delay over a far greater range. Furthermore the present technique allows polarization control. These features are essential to the present study.

Following transmission through a fused-silica window into an ultra-high vacuum chamber, the pump-probe

pulses are reflection focused with a silver-coated spherical mirror capable of supporting the bandwidth of our laser pulses without introducing group-velocity dispersion, as shown in Fig. 1. The laser focus is situated in the source region of a tightly apertured ($250\text{ }\mu\text{m}$) ion time-of-flight mass spectrometer (TOFMS) [20]. The aperture serves two purposes: to limit the angular acceptance (≤ 2 degrees for a 5.5 eV D^+ ion), and to dramatically limit the field of view of the spectrometer. By observing only the central $250\text{ }\mu\text{m}$ ‘slice’ of the $f/5$ focus, the instrument is sensitive only to those molecules exposed to a narrow intensity range. As a consequence, spatial integration over the focal volume is obviated, and the behaviour of the rotational wavepacket is clearly observed. This results in a remarkably high resolution measurement of the rotational wavepacket as compared to earlier observations.

Fig. 2(a) shows the measured rapid sequential ionization D^+ yield in false colour as a function of pump-probe delay (Δt , also referred to as evolution time) and D^+ ion kinetic energy; here, $\theta = \pi/2$. We are interested in the modulation in the SI yield $0 \leq \Delta t \leq 800\text{ fs}$, the signature of the revival of a rotational wavepacket in the D_2 molecule. Importantly, in Fig. 2, the orthogonality of the aligning pump pulse to the TOFMS (and probe polarization) axis results in the initial maximal alignment of the ensemble producing a minimum in the SI signal as the majority of the molecules are aligned perpendicular to the detector.

The solid circles in Fig. 2(b) represent the experimentally obtained high kinetic energy D^+ yield from the rapid SI of D_2 at small internuclear separation for $\theta = \pi/2$. The half- (280 fs) and full-revivals (560 fs) are clearly apparent in the results of both the integrated SI yield and the theoretical calculation, with excellent agreement observed between experiment and theory. At small delays $0 \leq \Delta t \leq 100\text{ fs}$, the discrepancy between experiment and theory is the result of the temporal wings of the pump and probe pulses overlapping to produce elliptical/circular polarization depending on Δt . When $\Delta t \geq 200\text{ fs}$, the time-dependent structure of the SI yield is purely the result of the rotational wavepacket.

In Fig. 2(b), between $200 \leq \Delta t \leq 800\text{ fs}$, there is evidence of fine structure in the experimentally observed wavepacket dependence, the result of the $1/4$, $1/2$ and $3/4$ revivals at respective fractions of $(2Bc)^{-1}$. Since the D^+ yield is recorded every 1 fs, an 11-point smoothing algorithm applied to the integrated SI yield (Fig. 2b) suppresses statistical fluctuations and hence enhances the fidelity of the fine structure observation without losing temporal resolution, as shown in Fig. 2(c).

Through the Fourier transform (FT) of the experimental signal (Fig. 2b), we recover the frequency components present in the rotational wavepacket. Fig. 2(d) and Fig. 2(e) show histograms of the FT of the calculation and the experimental data respectively, the peak positions corresponding to the dominant beat frequencies between

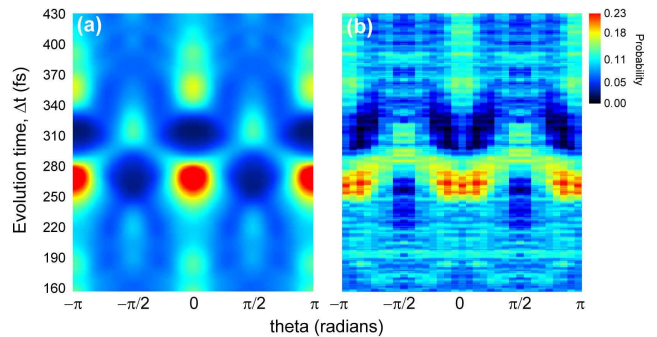


FIG. 3: (a) Simulated ‘quantum carpet’ [19] for an initially randomly aligned ensemble of room temperature D_2 molecules. For a particular Δt and θ , the false colour-scale indicates the wavepacket probability with a thermal average. In the range $230 \leq \Delta t \leq 290\text{ fs}$, the ensemble is predicted to be maximally aligned with the pump polarization direction. (b) The integrated rapid SI yield (normalized to the theory) over the same range of Δt indicates the theory describes our results with impressive accuracy: all the major features are reproduced.

rotational states. For a diatomic molecule, $\Delta J = 0, \pm 2$, thus the beat frequencies assigned to level J in Fig 2 are governed by the spacing between rotational levels J and $J+2$. The peak heights are proportional to the product of the respective quantum amplitudes. The nuclear spin statistics of D_2 are also evidenced by the domination of beats between even J states over odd J states.

The beats for $J = 0 - 2$, $1 - 3$ and $2 - 4$ occur at 5.5 THz, 9.1 THz and 12.8 THz respectively. Rather intriguingly, the recent work of Ergler *et al* [21], investigating vibrational wavepackets in the D_2^+ molecular ion, similar rotational components have been observed, and attributed to the creation of a rotational wavepacket in the molecular ion D_2^+ . However, the polarizability anisotropy and bond length change dramatically under ionization from D_2 to D_2^+ , with corresponding beat frequencies being a factor of two lower than in D_2 . The time-domain and equivalent FT frequency domain data described here are in excellent agreement with the expectation of impulsively excited rotational wavepackets formed in the neutral D_2 molecule.

The data presented in Fig. 2 describes only part of the rotational dynamics of D_2 as those molecules outside the angular acceptance of our detector simply are not detected. To fully understand the emergence of rotational order, we turn now to predicting and measuring the rapid variation of the angular distribution of molecules around the first half-revival. Fig. 3(a) is a false-colour representation of the expected probability distribution as a function of evolution time Δt and θ . When $250 \leq \Delta t \leq 280\text{ fs}$, maximal alignment is predicted: the ensemble is expected to be preferentially aligned in a narrow double-lobed distribution directed along $\theta = 0, \pi$ in this ‘quantum carpet’. By rotating θ over the range $-\pi$ to

π , the axis of revival of the rotational wavepacket is rotated with respect to our detector axis. The experimental data is shown in Fig. 3(b): the relative D^+ yield as a function of θ and Δt directly reflects the thermal average of the rotational wavepacket probability over the thermal average distribution of J . While some statistical scatter is present, the features of the quantum carpet are well resolved. This demonstrates how the molecular axes align through revival to create order. Up to $\simeq 190$ fs, the ensemble is to a large extent isotropic. However in the vicinity of the half revival, the rephasing of the wavepacket traps or confines the molecules in a well defined spatial distribution for a short period of time. It should be noted that the large energy spacing of the J-states in D_2 do not necessitate supersonic cooling, thus this demonstration of an ordered molecular ensemble illustrates a readily accessible quantum system.

The mapping of this ultrafast rotational wavepacket has a number of implications. On the most fundamental level, the observation of the quantum carpet in D_2 (confirmed by our theoretical predictions) illustrates that a room temperature ensemble of this theoretically important molecule can be organized into an ordered state. This can allow time- and energy-resolved measurements of the electronic and nuclear motion with spectroscopic accuracy. Considerable efforts are underway to perfect ultrashort (≤ 5 femtoseconds) pulse generation through molecular phase modulation [10]. By impulsively aligning a high pressure Raman-active gas (short rotational period makes D_2 a natural choice) in a hollow waveguide with an ultrafast pump pulse, a locally-aligned rotational revival propagates along the waveguide at the speed of light in the medium, and the molecular motion causes a strong phase modulation due to the refractive index change. A second pulse (directly equivalent to our probe) injected into the waveguide to coincide with the rotational revival is then spectrally broadened and compressed through the phase modulation. Importantly, it has been demonstrated that the time dependent phase introduced can be accurately controlled by changing the delay between the pump and probe pulses.

The experiment was carried out at the ASTRA Laser Facility, CCLRC Rutherford Appleton Laboratory, UK, where the assistance of J. M. Smith, E. J. Divall, K. Ertel,

O. Chekhlov, C. J. Hooker and S. Hawkes is gratefully acknowledged. This work was funded by the Engineering and Physical Sciences Research Council (UK). EMLE and JW acknowledge EPSRC studentships, JMcK and CRC wish to acknowledge funding from the Department of Employment and Learning (NI). RT acknowledges the Spanish Department of State of Education and Universities, and the European Social Fund.

* Electronic address: w.bryan@ucl.ac.uk

† Electronic address: i.williams@qub.ac.uk

‡ Electronic address: w.r.newell@ucl.ac.uk

- [1] R. W. Taft Jr., *Steric Effects in Organic Chemistry* (Wiley, New York), (1956).
- [2] H. J. Loesch and A. Remscheid, *J. Chem. Phys.* **93** 4779 (1990).
- [3] M. Wu, R. J. Bemish and R. E. Miller, *J. Chem. Phys.* **101** 9447 (1994).
- [4] H. Stapelfelt and T. Seideman, *Rev. Mod. Phys.* **75** 543 (2003).
- [5] T. Seideman, *Phys. Rev. Lett.* **83** 4971 (1999).
- [6] P. W. Dooley *et. al*, *Phys. Rev. A* **68** 023406 (2003).
- [7] E. Peronne *et. al*, *Phys. Rev. Lett.* **91** 043003 (2003).
- [8] J. Itatani *et. al*, *Nature (London)* **432** 867 (2004).
- [9] T. Kanai, S. Minemoto and H. Sakai, *Nature (London)* **435** 470 (2005).
- [10] V. Kalosha, M. Spanner, J. Herrman and M. Ivanov, *Phys. Rev. Lett.* **88** 103901 (2002).
- [11] X. M. Tong and C. D. Lin, *Phys. Rev. A* **70** 023406 (2004).
- [12] B. Friedrich and D. Herschbach, *Phys. Rev. Lett.* **74** 4623 (1995).
- [13] M. Spanner, E. A. Shapiro and M. Ivanov, *Phys. Rev. Lett.* **92** 093001 (2004).
- [14] K. F. Lee, D. M. Villeneuve, P. B. Corkum and E. A. Shapiro, *Phys. Rev. Lett.* **93** 233601 (2004).
- [15] V. Renard *et. al*, *Phys. Rev. A* **70** 033420 (2004).
- [16] N. Xu *et. al*, *Opt. Express* **14** 4992 (2006).
- [17] F. Rosca-Pruna and M. J. J. Vrakking, *Phys. Rev. Lett.* **87** 153902 (2001).
- [18] K. F. Lee, F. Legare, D. M. Villeneuve and P. B. Corkum, *J. Phys. B* **39** 4081 (2006).
- [19] R. Torres, R. de Nalda and J. P. Marangos, *Phys. Rev. A* **72** 023420 (2005).
- [20] J. McKenna *et. al*, *J. Mod. Opt.* **in print** (2007).
- [21] Th. Ergler *et. al*, *Phys. Rev. Lett.* **97** 193001 (2006).